Available online at www.sciencedirect.com
ScienceDirect
Nuclear Physics A 956 (2016) 348–351
NUCLEAR PHYSICS A
www.elsevier.com/locate/nuclphysa

Indications for a critical point in the phase diagram for hot and dense nuclear matter

Roy A. Lacey

Depts. of Chemistry & Physics, Stony Brook University, NY 11794

Abstract

Two-pion interferometry measurements are studied for a broad range of collision centralities in Au+Au ($\sqrt{s_{NN}} = 7.7 - 200$ GeV) and Pb+Pb ($\sqrt{s_{NN}} = 2.76$ TeV) collisions. They indicate non-monotonic excitation functions for the Gaussian emission source radii difference ($R^2_{\rm out} - R^2_{\rm side}$), suggestive of reaction trajectories which spend a fair amount of time near a soft point in the equation of state (EOS) that coincides with the critical end point (CEP). A Finite-Size Scaling (FSS) analysis of these excitation functions, provides further validation tests for the CEP. It also indicates a second order phase transition at the CEP, and the values $T^{\rm cep} \sim 165$ MeV and $\mu_B^{\rm cep} \sim 95$ MeV for its location in the (T, μ_B)-plane of the phase diagram. The static critical exponents ($\nu \approx 0.66$ and $\gamma \approx 1.2$) extracted via the same FSS analysis, place this CEP in the 3D Ising model (static) universality class. A Dynamic Finite-Size Scaling analysis of the excitation functions, gives the estimate $z \sim 0.87$ for the dynamic critical exponent, suggesting that the associated critical expansion dynamics is dominated by the hydrodynamic sound mode.

Keywords: critical point, phase transition, static critical exponents, dynamic critical exponent

1. Introduction

A major goal of the worldwide program in relativistic heavy ion research, is to chart the phase diagram for nuclear matter [1, 2, 3, 4]. Pinpointing the location of the phase boundaries and the critical end point (CEP), in the plane of temperature (T) versus baryon chemical potential (μ_B), is key to this mapping. Full characterization of the CEP not only requires its location, but also the static and dynamic critical exponents which classify its critical dynamics and thermodynamics, and the order of the associated phase transition.

Current theoretical guidance indicates that the CEP belongs to the 3D-Ising [or Z(2)] static universality class with the associated critical exponents $\nu \approx 0.63$ and $\gamma \approx 1.2$ [4, 5]. However, the predictions for its location span a broad swath of the (T, μ_B)-plane, and do not provide a consensus on its location [4]. A recent study which takes account of the non-linear couplings of the conserved densities [6] suggests that the CEP's critical dynamics may be controlled by three distinct slow modes, each characterized by a different value of the dynamic critical exponent z; a thermal mode ($z_T \sim 3$), viscous mode ($z_v \sim 2$) and a sound mode ($z_s \sim -0.8$). The phenomena of critical slowing down results from $z > 0$. The predicted negative value for z_s could have profound implications for the CEP search since it implies critical speeding-up for critical reaction dynamics involving *only* the sound mode. The present-day theoretical challenges emphasize the need for detailed experimental validation and characterization of the CEP.

http://dx.doi.org/10.1016/j.nuclphysa.2016.01.032

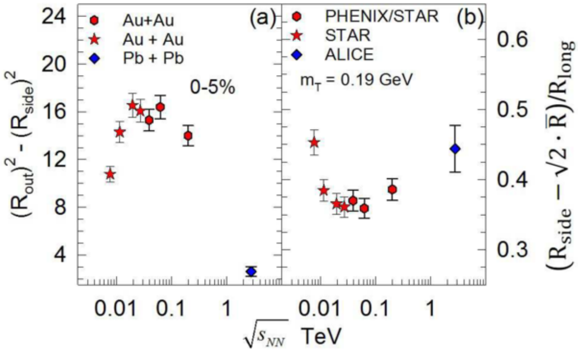

Fig. 1: (Color online) The $\sqrt{s_{NN}}$ dependence of (a) $(R^2_{out} - R^2_{side})$, and (b) $[(R_{side} - \sqrt{2}\bar{R})/R_{long}]$ [8].

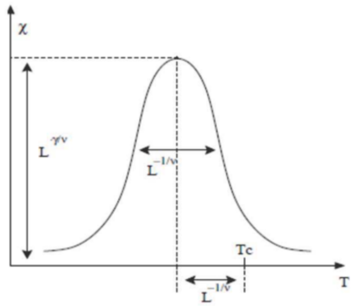

Fig. 2: Illustration of the Finite-Size (L) dependence of the peak position, width and magnitude of the susceptibility χ (see text).

2. Anatomy of the search strategy for the CEP

The critical point is characterized by several (power law) divergences linked to the divergence of the correlation length $\xi \propto |t|^{-\nu} \equiv |T - T^{\rm cep}|^{-\nu}$. Notable examples are the baryon number fluctuations $\langle(\delta n)\rangle \sim \xi^{\gamma/\nu}$, the isobaric heat capacity $C_p \sim \xi^{\gamma/\nu}$ and the isothermal compressibility $\kappa_T \sim \xi^{\gamma/\nu}$. Such divergences suggest that reaction trajectories which are close to the CEP, could drive anomalies in the reaction dynamics to give distinct non-monotonic patterns for the related experimental observables. Thus, a current experimental strategy is to carry out beam energy scans which enable a search for non-monotonic excitation functions over a broad domain of the (T, μ_B)-plane. In this work we use the non-monotonic excitation functions for HBT radii combinations that are sensitive to the divergence of the compressibility [7].

The expansion of the pion emission source produced in heavy ion collisions, is driven by the sound speed $c_s^2 = 1/\rho\kappa_s$, where ρ is the density, $\kappa_s = \varsigma\kappa_T$ is the isentropic compressibility and $\varsigma = C_v/C_p$ is the ratio of the isochoric and isobaric heat capacities. Thus, an emitting source produced in the vicinity of the CEP, would be subject to a precipitous drop in the sound speed and the collateral increase in the emission duration [9], which results from the divergence of the compressibility. The space-time information associated with these effects, are encoded in the Gaussian HBT radii which serve to characterize the emission source. That is, $R_{\rm long}$ is related to the source lifetime τ, $(R^2_{\rm out} - R^2_{\rm side})$ is sensitive to its emission duration $\Delta\tau$ [10] (an intensive quantity) and $[(R_{\rm side} - \sqrt{2}\bar{R})/R_{\rm long}]$ gives an estimate for its expansion speed (for small values of m_T), where $\bar{R}$ is an estimate of the initial transverse size, obtained via Monte Carlo Glauber model calculations [8, 7]. Therefore, characteristic convex and concave shapes are to be expected for the non-monotonic excitation functions for $(R^2_{\rm out} - R^2_{\rm side})$ and $[(R_{\rm side} - \sqrt{2}\bar{R})/R_{\rm long}]$ respectively.

These predicted patterns are validated in Figs. 1(a) and (b). They reenforce the connection between $(R^2_{\rm out} - R^2_{\rm side})$ and the compressibility and suggest that reaction trajectories spend a fair amount of time near a soft point in the EOS that coincides with the CEP. We associate $(R^2_{\rm out} - R^2_{\rm side})$ with the susceptibility κ and employ Finite-Size Scaling (FSS) for further validation tests, as well as to extract estimates for the location of the CEP and the critical exponents which characterize its static and dynamic properties.

3. Characterization of the CEP via Finite-Size Scaling

For infinite volume systems, ξ diverges near $T^{\rm cep}$. Since $\xi \leq L$ for a system of finite size L^d (d is the dimension), only a pseudo-critical point, shifted from the genuine CEP, is observed. This leads to a characteristic set of Finite-Size Scaling (FSS) relations for the magnitude ($\chi_T^{\rm max}$), width (δT) and peak position (t_T) of the susceptibility [7] as illustrated in Fig. 2; $\chi_T^{\rm max}(V) \sim L^{\gamma/\nu}$, $\delta T(V) \sim L^{-1/\nu}$ and $t_T(V) \sim T^{\rm cep}(V) - T^{\rm cep}(\infty) \sim L^{-1/\nu}$. It also leads to the scaling function $\chi(T, L) = L^{\gamma/\nu} P_\chi(tL^{1/\nu})$, which results in data collapse onto a single curve for robust values of $T^{\rm cep}$, $\mu_B^{\rm cep}$ and the critical exponents ν and γ.